Annals of Botany **00**: 1–12, 2026
https://doi.org/10.1093/aob/mcag343, available online at www.academic.oup.com/aob

ANNALS OF BOTANY
Nonprofit since 1887

Downloaded from academic.oup.com/aob/advance-article/doi/10.1093/aob/mcag343/9002709 by National Science & Technology Library user on 24 November 2026

ORIGINAL ARTICLE

Nitrogen supply and neighbour identity shape responses to below-ground interactions in a cultivated rice genotype and its wild relative

Weila Cheng[1], Xianke Yang[1], Xiaoxia Ling[1], Fei Wang[1], Jianguo Man[1], Zhenmei Wang[1], Kehui Cui[1,*], Jianliang Huang[1,*], Shaobing Peng[1,*] and Dongliang Xiong[1,*]

[1]*National Key Laboratory of Crop Genetic Improvement, Hubei Hongshan Laboratory, MARA Key Laboratory of Crop Ecophysiology and Farming System in the Middle Reaches of the Yangtze River, Huazhong Agricultural University, Wuhan, Hubei 430070, China*
[*]*For correspondence. E-mail dlxiong@mail.hzau.edu.cn*

Received: 27 April 2026 Returned for revision: 06 September 2026 Accepted: 20 October 2026

• **Background and Aims** The outcomes of below-ground interactions depend on resource availability and neighbour identity, but how these factors jointly affect plant performance across planting contexts remains unclear. We tested how nitrogen (N) supply and neighbour identity affected responses to below-ground interactions in a cultivated rice genotype and its wild relative grown in monocultures or mixtures. We examined whether interaction outcomes differed between intra- and interspecific neighbour treatments, whether low N increased asymmetry between the two rice species in biomass allocation and N acquisition, and whether these whole-plant responses corresponded with leaf physiological traits.
• **Methods** Plants were grown under low and high N supply in monocultures and mixtures, with adjacent root compartments separated either by a permeable mesh barrier or an impermeable plastic barrier. We used the relative interaction index (RII) to quantify mesh–plastic differences in biomass production and allocation, root biomass components, N accumulation and leaf physiological traits; positive RII estimates indicate higher trait values under the mesh treatment, negative estimates indicate lower values, and estimates near zero indicate little difference between barrier treatments.
• **Key results** Responses to mesh-mediated below-ground interactions depended on neighbour identity and N availability. RII estimates were close to zero or positive in some monocultures but predominantly negative in mixtures. Within mixtures, the *O. sativa* genotype 'Huanghuazhan' better maintained whole-plant performance, whereas the *O. nivara* accession showed larger trait reductions. This divergence was most apparent under low N. Leaf physiological responses did not consistently parallel the cumulative changes in whole-plant traits.
• **Conclusions** These results indicate that N supply and neighbour identity modulate divergent responses to mesh-mediated below-ground interactions between a cultivated rice genotype and its wild relative. Because this study compared one cultivated rice genotype with one wild relative, broader genotype sampling will be needed to test whether these patterns reflect domestication-associated divergence.

Key words: Below-ground interactions, rice domestication, wild relative, whole-plant traits, nitrogen availability, *Oryza sativa* ssp. *indica* 'Huanghuazhan', *Oryza nivara*.

INTRODUCTION

Plant performance in dense stands depends not only on intrinsic growth capacity but also on interactions with neighbouring plants (Anten and Chen, 2021; Mazal *et al.*, 2023). Below-ground interactions are especially important because roots determine access to soil resources and mediate local nutrient depletion, resource redistribution and chemical signalling among plants (Biedrzycki and Bais, 2010; Semchenko *et al.*, 2014; Zhu *et al.*, 2022). The presence of a neighbouring root system can therefore alter plant growth, biomass allocation and nutrient acquisition even when direct root intermingling is prevented (Zhu *et al.*, 2019*a*; Chen *et al.*, 2021; Yang *et al.*, 2024). These effects are not uniformly competitive. Depending on environmental conditions and the identities of the interacting plants, below-ground interactions may produce negative, neutral or positive growth responses (Anten and Chen, 2021).

Nitrogen (N) availability is likely to influence below-ground interaction outcomes (De Tombeur *et al.*, 2022; Yang *et al.*, 2024). Under low N, plants commonly adjust root growth, biomass allocation and nutrient uptake in

© The Author(s) 2026. Published by Oxford University Press on behalf of the Annals of Botany Company. All rights reserved. For commercial re-use, please contact reprints@oup.com for reprints and translation rights for reprints. All other permissions can be obtained through our RightsLink service via the Permissions link on the article page on our site—for further information please contact journals.permissions@oup.com.

ways that increase soil exploration or N acquisition (Kiba and Krapp, 2016). Resource limitation may therefore intensify below-ground competition because neighbouring plants depend more strongly on a restricted nutrient supply. However, the direction and magnitude of the response may also depend on whether the neighbour is conspecific or heterospecific (Yang *et al.*, 2018; Xu *et al.*, 2021). Conspecific neighbours may overlap more strongly in their resource requirements and acquisition strategies, potentially producing relatively symmetrical responses (Jaafry *et al.*, 2019). Heterospecific neighbours, by contrast, may differ in root allocation, nutrient demand, uptake capacity or plasticity, resulting in asymmetrical interaction outcomes (Xu *et al.*, 2012; Ehlers and Bilde, 2019; Zhu *et al.*, 2022). Nitrogen addition may further modify these relationships by relaxing nutrient limitation or changing the relative effectiveness of contrasting resource acquisition strategies (Minden and Olde Venterink, 2019; Yang *et al.*, 2024). Below-ground interaction outcomes therefore cannot be predicted from N availability or neighbour identity alone. Crop domestication and breeding have altered plant architecture, resource allocation and population-level performance under managed, high-density conditions (Weiner *et al.*, 2017; Zhu *et al.*, 2019*b*). These changes may also have modified how cultivated plants respond to neighbours (Zhu *et al.*, 2019*a*). Selection for high stand productivity is often expected to reduce investment in traits that increase individual resource pre-emption, whereas wild relatives may retain greater plasticity in resource foraging under heterogeneous conditions (Donald, 1968; Montazeaud *et al.*, 2020). However, domestication has not affected root systems uniformly across crop species (Martín-Robles *et al.*, 2019). Comparative evidence indicates that some cultivated plants retain or have acquired root traits associated with effective nutrient capture, including greater soil exploration or enhanced nutrient acquisition under nutrient limitation (Martín-Robles *et al.*, 2019; Perkins and Lynch, 2021; Odone and Thorup-Kristensen, 2025). Cultivated and wild plants may therefore differ in their below-ground strategies without conforming to a simple contrast between weak and strong competitiveness.

These contrasting selection histories raise the question of whether cultivated and wild plants respond differently to conspecific and heterospecific neighbours, particularly when soil N is limiting. Rice can modify root growth in response to neighbour identity, including kinship and genotype composition (Semchenko *et al.*, 2014; Yang *et al.*, 2018), but whether these context-dependent responses differ between cultivated rice and its wild relatives remains unclear. It is also unclear whether low N increases asymmetry between cultivated and wild varieties in biomass allocation and N acquisition. Addressing these questions requires comparisons of intra- and interspecific neighbour effects under contrasting N supplies.

Below-ground interaction outcomes may also differ across temporal and organizational scales (Wang *et al.*, 2021; Carter *et al.*, 2025). Biomass production, biomass allocation and N accumulation integrate resource acquisition and partitioning over the growth period, whereas gas exchange and related leaf traits characterize physiological status at the time of measurement (Mahaut *et al.*, 2023; Lai *et al.*, 2026; Wang *et al.*, 2026). Responses at these scales may not vary in parallel (Bebout *et al.*, 2026). Assessing both sets of traits can therefore show whether cumulative changes in plant growth and N economy are accompanied by corresponding adjustments in leaf physiology. Here, this cross-scale comparison was used as a complementary assessment of interaction outcomes rather than as a test of whether one trait class provides a better indicator of plant performance.

In this study, we compared a cultivated rice genotype, *Oryza sativa* subsp. *indica* 'Huanghuazhan' (referred to hereafter as *O. sativa*), with its wild relative, *Oryza nivara*. Plants were grown under low- and high-N supply with either a conspecific or heterospecific neighbour. Below-ground interactions were manipulated using either a permeable mesh barrier, which prevented root intermingling but allowed diffusive exchange between root compartments, or an impermeable plastic barrier, which isolated the two root compartments. We quantified interaction outcomes at the pot and individual plant scales using biomass production, biomass allocation, root biomass components, organ level N accumulation and leaf physiological traits. We addressed three questions: (1) how N supply and neighbour identity affected the direction and magnitude of responses to mesh-mediated below-ground interactions; (2) whether low N increased asymmetry between the *O. sativa* genotype and the *O. nivara* accession, particularly when they were grown together; and (3) whether changes in cumulative biomass allocation and N acquisition were accompanied by corresponding changes in leaf physiological traits.

MATERIALS AND METHODS

Plant materials

Oryza sativa and *O. nivara* were used as experimental materials. *Oryza sativa* seeds were sourced from a local commercial supplier. The *O. nivara* used in the experiment is single-genotype material sourced from the National Wild Rice Germplasm Bank (Guangzhou, China). Seedlings were raised under indoor nursery conditions and transplanted 22 d after sowing. Leaf physiological measurements were conducted before harvest; photosynthetic response curves were measured 40–63 d after transplanting and other leaf physiological traits were measured 58–63 d after transplanting. All plants were harvested 65 d after transplanting.

The high cohesiveness and viscosity of paddy soil typically hinder the recovery of complete, undamaged root systems during harvest. To facilitate intact root sampling, field-collected paddy soil was air-dried and mechanically ground prior to use. Quartz sand was then mixed thoroughly with the dried soil at a mass ratio of 9:5 (paddy soil:quartz sand), yielding a less compact growth substrate better suited for root excavation and morphological assessments.

Experimental set-up for below-ground interactions

To assess both interspecific and intraspecific below-ground interactions, 5.0-L plastic pots were longitudinally divided into two compartments, each containing 2.3 kg of dry soil–sand mixture (see details above). One rice seedling

Downloaded from academic.oup.com/aob/advance-article/doi/10.1093/aob/mcag343/9002709 by National Science & Technology Library user on 24 November 2026

was transplanted into each compartment, with an interplant distance of 15 cm within a pot (Supplementary Data Fig. S1A). Planting treatments were designed to simulate different scenarios of root interaction.

Two barrier treatments were implemented to manipulate below-ground interactions between the two root compartments. In the mesh treatment, the compartments were separated by a permeable nylon mesh with a pore size of 50 μm. The mesh prevented direct root intermingling and occupation of the same soil microsites but permitted diffusion of water, dissolved nutrients and soluble root-derived compounds between compartments. In the plastic treatment, an impermeable polytetrafluoroethylene (PTFE) film prevented both root contact and diffusive exchange between the two root compartments (Supplementary Data Fig. S1B). The plastic treatment therefore provided a root zone isolation reference rather than a neighbour-free or no-competition control.

Within both mesh and plastic treatment frameworks, planting compositions were established to represent different competitive contexts. In the monoculture composition (conspecific neighbour), two arrangements were used: *O. sativa* paired with *O. sativa*, and *O. nivara* paired with *O. nivara*. In the mixture composition (heterospecific neighbour), one compartment was planted with *O. sativa* and the other with *O. nivara*. Each of the three planting compositions was subjected to both mesh and plastic treatments.

Nitrogen treatments

Two N supply levels were imposed in combination with two root barrier treatments and two planting compositions, resulting in 12 distinct potted experimental conditions in total (Supplementary Data Table S1). For each condition, ten replicate pots were prepared. The low N treatment received no supplementary N, whereas the high N treatment received a total of 1.4 g N per pot compartment. For the high N treatment, urea was dissolved in water and applied to each compartment at 3-week intervals during the growth period. Nitrogen application ceased 1 week prior to gas exchange measurements. Unlike N, both phosphorus (P) and potassium (K) were incorporated directly into the soil–sand mixture before pot filling, at a rate of 0.15 g per kilogram of substrate. Throughout the experiment, pots were regularly and randomly rearranged to minimize positional effects, following standard experimental practice.

Nitrogen content

Prior to mixing the quartz sand into the growth substrate, dry paddy soil was sampled (three replicates) to determine its initial nutrient status. Soil aggregates were gently crushed and were passed through a 150-μm sieve to remove stones and organic debris before chemical analysis.

For nutrient determination, ∼0.2 g of sieved soil was weighed into a 100-mL digestion tube, and 5 mL of concentrated sulfuric acid was added. Samples were digested at 320 °C for ∼3 h until the solution became transparent. During digestion, five drops of hydrogen peroxide were added at 20-min intervals to ensure complete oxidation. After digestion, the entire contents of the tube, including any residues, were transferred to a 100-mL volumetric flask. The flask was then brought to volume with distilled water and allowed to stand for at least 12 h. The supernatant was subsequently transferred into disposable tubes and diluted 10-fold for subsequent chemical analysis.

Total N concentrations were quantified using a discrete wet chemistry analyser (SmartChem 200, AMS-Westco, Rome, Italy). The initial paddy soil contained 1.53 mg g^{-1} total N.

Light response curve

Light response curves were measured on four plants per treatment combination ($n = 4$), using one newly fully expanded leaf per plant. Gas exchange and chlorophyll fluorescence measurements were conducted using a LI-6800 portable photosynthesis system (LI-COR, Lincoln, NE, USA). To minimize environmental variation, plants were transferred to a walk-in growth chamber (GR48, Conviron, Canada) 1 d before measurements. The growth chamber was set at 28 °C (day) and 24 °C (night), 65 % relative humidity, and a leaf-level irradiance of ∼400 μmol m^{-2} s^{-1} during the daytime. During light response curve measurements, temperature in the LI-6800 cuvette was maintained at 28 °C, reference CO_2 concentration at 400 μmol mol^{-1} and relative humidity at 65 %. Leaves were acclimated to a photosynthetic photon flux density (PPFD) of 1500 μmol m^{-2} s^{-1} until the net photosynthetic rate (A) stabilized (typically 15–30 min). The LI-6800 auto-programme then stepped PPFD through the following sequence at intervals of 60–90 s: 2000, 1500, 1200, 1000, 800, 600, 400, 200, 150, 100, 50 and 0 μmol m^{-2} s^{-1}. Steady-state fluorescence (F_s) and maximum light-adapted fluorescence (F_m') were recorded at each step. Light response curves were fitted using a non-rectangular hyperbola model:

$$A = \frac{(\Phi \cdot PPFD + A_{max}) - \sqrt{(\Phi \cdot \mathrm{PPFD} + A_{max})^2 - 4 \cdot \theta \cdot \Phi \cdot \mathrm{PPFD} \cdot A_{max}}}{2 \cdot \theta} - R_d$$

where Φ is the apparent quantum yield, A_{max} is maximum gross photosynthesis, θ is the curvature factor and R_d is daytime respiration rate.

CO_2 response curve

CO_2 response (A–C_i) curves were measured on four plants per treatment combination ($n = 4$), using one newly fully expanded leaf per plant, under the same environmental conditions used for light response curves. Based on preliminary light response results, photosynthesis of both species reached ∼75 % saturation at ∼1000 μmol m^{-2} s^{-1}; therefore, a PPFD of 1500 μmol m^{-2} s^{-1} was used for A–C_i curves. After leaves had reached a steady photosynthetic rate at 400 μmol mol^{-1} CO_2 and 1500 μmol m^{-2} s^{-1} PPFD, the CO_2 concentration was sequentially adjusted to 400, 300, 200, 100, 50, 400, 600, 800, 1000, 1200, 1500 and 2000 μmol mol^{-1} with 150–240 s between steps. The first measurement in each curve was used as the steady-state gas exchange value.

Downloaded from academic.oup.com/aob/advance-article/doi/10.1093/aob/mcag343/9002709 by National Science & Technology Library user on 24 November 2026

Mesophyll conductance

The actual quantum efficiency of photosystem II (Φ_{PSII}) and electron transport rate (J) were calculated as:

$$\Phi_{PSII} = \frac{F'_m - F_s}{F'_m}$$

$$J = \Phi_{PSII} \times PPFD \times \alpha\beta$$

where α is leaf absorbance and β is the partitioning of absorbed quanta between PSI and PSII. Following Xiong *et al.* (2015, 2017), $\alpha\beta$ was set to 0.425.

Chloroplast CO_2 concentration (C_c) and mesophyll conductance (g_m) were estimated using the 'variable J' method:

$$C_c = \frac{\Gamma^*(J + 8(A + R_d))}{J - 4(A + R_d)}$$

$$g_m = \frac{A}{C_i - C_c}$$

where A and C_i were taken directly from steady-state gas exchange. The CO_2 compensation point in the absence of respiration (Γ^*) was set to 40 μmol mol^{-1}, the typical value for rice (Xiong *et al.*, 2015, 2017). R_d was obtained from light response curve fitting.

SPAD and leaf trait measurement

Following completion of the A–C_i curve measurements, SPAD readings were obtained on the same leaves using a SPAD-502. Leaf length was measured with a ruler, and leaf width was measured with a vernier calliper. Leaves were then excised, flattened and photographed from a top-down perspective. Leaf area was quantified from these images using ImageJ (National Institutes of Health, Bethesda, MD, USA). After imaging, leaves were oven-dried at 80 °C until constant mass, and dry weight was recorded.

Plant sampling and root scanning

Six individual plants were harvested per treatment. For mixtures, these six plants originated from six independent pots, whereas for monocultures six plants were harvested from three pots. After harvest, plants were thoroughly washed to remove soil residues. Plant height and tiller number were recorded, and each plant was separated into roots, stems and leaves. Total leaf area per plant was measured using an LI-3100C bench-top leaf area meter (LI-COR, Lincoln, NE, USA).

Root images were acquired using an Epson Perfection V700 Photo scanner (Seiko Epson Corporation, Japan) at 300 dpi and analysed using WinRHIZO (version 2003b, Regent Instruments Inc.). Because very fine roots could not be reliably resolved at this resolution and were difficult to separate without substantial measurement error, no diameter-based detection threshold was applied. Following published rice root classification criteria (Coudert *et al.*, 2010), the embryonic radicle and nodal crown roots were separated from lateral roots and scanned, whereas lateral roots were excluded from image-based morphological analysis. Scanned traits included scanned axial root length, scanned axial root surface area, mean diameter of scanned axial roots, scanned axial root volume and tip number of the scanned root fraction.

The scanned axial root fraction and the unscanned lateral root fraction were oven-dried separately at 80 °C and weighed. Total root biomass was calculated as the sum of the dry masses of the two root fractions. Stems and leaves were also oven-dried at 80 °C and weighed separately. Ground root, stem and leaf samples were digested using the procedure described for soil samples, and total N content was determined using the same analytical method.

Statistical analysis

The relative interaction index (RII) was calculated as RII $= (X_{mesh} - X_{plastic})/(X_{mesh} + X_{plastic})$, where X_{mesh} and $X_{plastic}$ denote the trait values under the permeable mesh barrier and impermeable plastic barrier treatments, respectively. RII was estimated separately for each treament at pot and plant level. Uncertainty in RII was estimated using a stratified, unpaired cluster bootstrap at the pot level. Because mesh and plastic pots were independently established and no predefined pairing or blocking relationship existed between them, the two barrier treatments were resampled independently. For plant-level traits in monocultures, measurements from the two conspecific plants were averaged within each pot before resampling. For mixture pots, the observations of the two species from the same pot were retained as a cluster and resampled together. Pot-level traits were resampled directly from the raw pot totals.

In each of 10 000 bootstrap iterations, pots were sampled with replacement within each species combination × N supply × root barrier stratum while retaining the original number of pots. Species-specific means were then calculated for plant-level traits, and the means of the resampled mesh and plastic groups were used to calculate RII. Percentile 95 % confidence intervals were obtained from the bootstrap distributions. An RII confidence interval excluding zero indicated a difference between the mesh and plastic treatments within the corresponding treatment combination; it did not by itself identify the biological mechanism underlying that difference.

Absolute trait values were analysed separately from the RII estimates. Pot-level total biomass was analysed using a Gaussian linear model with species combination, N supply, root barrier treatment and all interactions among these factors as fixed effects: pot total biomass ~ species combination × N supply × barrier. Because each pot contributed one pot-level observation, pot identity was the experimental unit and was not included as an additional random effect. Plant-level traits, including organ and total biomass, root-to-shoot ratio, root biomass components, organ-level and total N accumulation, and leaf physiological traits, were analysed separately using linear mixed-effects models: trait ~ species × planting composition × N supply × barrier + (1 | pot identity).

Pot identity was included as a random intercept to account for the non-independence of plants grown in the same pot. Individual plant was not included as a random effect because each response variable was measured once per

Downloaded from academic.oup.com/aob/advance-article/doi/10.1093/aob/mcag343/9002709 by National Science & Technology Library user on 24 November 2026

plant. Categorical predictors were coded using sum-to-zero contrasts, and fixed effects were evaluated using Type III tests with Satterthwaite's approximation for denominator degrees of freedom. Formal tests of whether the root barrier effect depended on species, N supply or planting composition were based on the corresponding interaction terms in these models and were conducted on the absolute trait scale.

Planned mesh–plastic contrasts were obtained from estimated marginal means within each species combination × N supply treatment for pot-level biomass and within each species × planting composition × N supply treatment for plant-level traits. Contrasts were expressed as mesh minus plastic, and *P*-values were adjusted using the Holm method across barrier contrasts within each response trait. Model assumptions were assessed using quantile–quantile plots of residuals and plots of residuals against fitted values. Models were fitted using all available observations for each response variable, and missing values were not imputed.

To summarize covariation among traits, we performed principal component analysis (PCA) on absolute trait values using complete cases. The observational unit was the pot–species combination. For monocultures, measurements from the two conspecific plants were averaged within each pot, whereas species-specific observations were retained for mixtures. All pot-level values derived from the above processing were subjected to log(x) transformation, followed by centring and scaling before PCA computation. The PCA included 14 whole-plant, root and leaf traits, including total biomass, total N accumulation, leaf area per plant, root-to-shoot ratio, the scanned axial root biomass, the unscanned lateral root biomass, scanned axial root length, mean diameter of scanned axial roots, tip number of the scanned root fraction, A, SPAD, stomatal conductance (g_s), maximum carboxylation rate (V_{cmax}) and maximum electron transport rate (J_{max}).

All data processing and statistical analyses were conducted using Microsoft Excel 2021 and R version 4.3.2. All graphical outputs were produced in R using the ggplot2 package. Linear mixed-effects models were fitted using the lmer function in the lmerTest package, with *P*-values for fixed effects calculated using Satterthwaite's approximation for denominator degrees of freedom. The PCA analysis was conducted using the prcomp function in R. Light response curves were fitted using the non-rectangular hyperbola model implemented with the orthogonal non-linear least-squares regression (onls) method in R. The A–C_i curves were fitted using the plantecophys package, from which V_{cmax} and J_{max} were estimated. Statistical significance was set at $P < 0.05$.

RESULTS

Baseline growth and biomass allocation across species and N supply

Both rice types produced more biomass under high N than under low N, although the magnitude of this response differed between them (Supplementary Data Fig. S2; Supplementary Data Tables S2 and S3). Species identity significantly affected leaf, stem and root biomass (leaf: $P = 0.003$; stem and root: $P < 0.001$; Supplementary Data Table S3), and the significant species × N supply interaction for root biomass ($P = 0.001$) indicated contrasting root growth responses to N availability. *Oryza nivara* also had a consistently higher root-to-shoot ratio than *O. sativa* (Supplementary Data Fig. S3; Supplementary Data Table S2), although this difference varied with N availability (species × N supply interaction, $P < 0.001$; Supplementary Data Table S3).

Pot- and plant-level growth response to mesh-mediated below-ground interactions

Mesh-mediated below-ground interactions affected plant growth differently across N supply levels and planting compositions (Fig. 1). Estimates of RII varied among species combinations and N treatments (Fig. 1A). Under high N, total biomass was higher in the mesh than in the plastic treatment for *O. sativa* monocultures, whereas *O. nivara* monocultures showed little difference between barrier treatments. In mixtures, total biomass was lower under the mesh treatment than under the plastic treatment, with more negative RII estimates under low N than under high N (Fig. 1A). Patterns at the individual plant level were broadly consistent with those at the pot level, although responses differed between the two rice types (Fig. 1B). In *O. sativa* monocultures, biomass RII was positive under high N but negative under low N. In *O. nivara* monocultures, RII remained close to zero under both N levels. In mixtures, biomass RII estimates for both rice types were below zero under both N levels.

Root barrier treatment affected leaf biomass ($P = 0.02$) and stem biomass ($P = 0.01$), but not root biomass ($P = 0.388$; Supplementary Data Table S3). Several interaction terms further suggested that the effect of the root barrier depended on growth context, particularly for leaf biomass, stem biomass, root biomass across planting compositions (planting composition × barrier, all $P < 0.05$), and for stem biomass the three-way interaction of planting composition × N supply × barrier were significant ($P = 0.002$). Consistent with these ANOVA results, Holm-adjusted planned contrasts revealed significant differences in organ biomass between mesh and plastic treatments only within specific species × N supply × planting composition combinations, instead of being observed universally across all treatment groups (Supplementary Data Table S2).

Biomass allocation and root architectural traits underlying interaction outcomes

At the whole-plant level, interaction effects on biomass allocation were reflected in shifts in the root-to-shoot ratio (Fig. 2A). In monocultures, *O. sativa* showed contrasting responses across N supply levels. Under low N, positive RII estimates for the root-to-shoot ratio indicated greater relative root allocation under the mesh treatment than under the plastic treatment. Under high N, RII estimates were slightly negative, with little evidence of a marked shift in relative root allocation. In contrast, *O. nivara* showed a significant positive response under high N but a negative response under low N. In mixed plantings, the two species responded differently. In mixtures, RII estimates for relative root

Downloaded from academic.oup.com/aob/advance-article/doi/10.1093/aob/mcag343/9002709 by National Science & Technology Library user on 24 November 2026

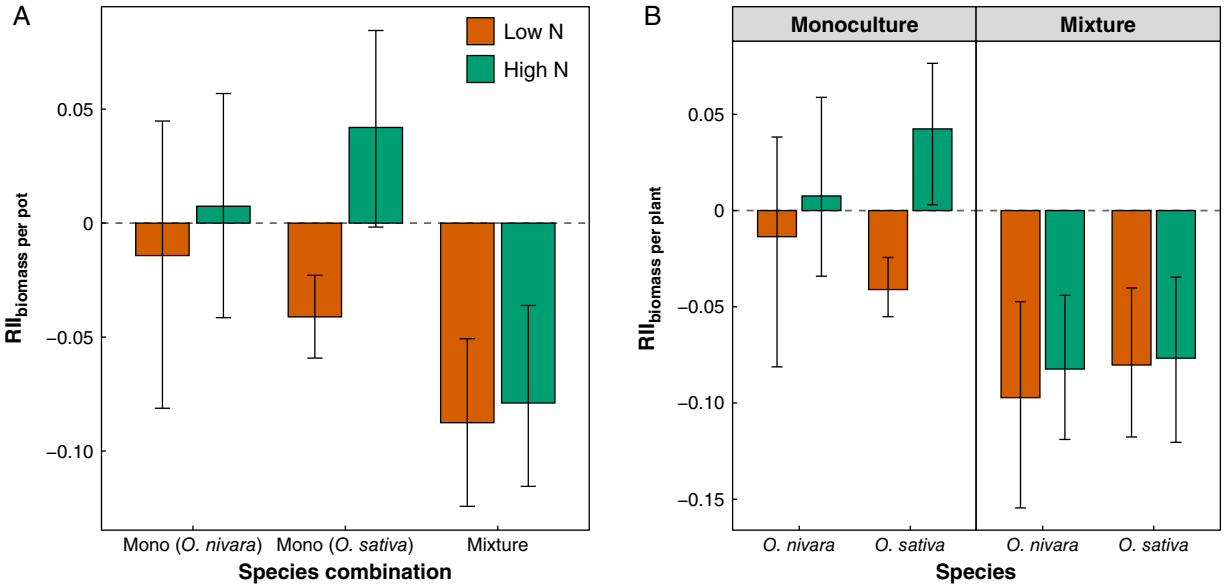


FIG. 1. Relative interaction index (RII) at pot and individual plant scales under contrasting N conditions. (A) Pot-level RII of total biomass for three species combinations (monoculture of *O. nivara*, monoculture of *O. sativa*, mixture of *O. nivara* and *O. sativa*) under low- and high-N conditions. (B) Plant-level RII of total biomass for *O. sativa* and *O. nivara* grown under low and high N conditions. The index was calculated as $RII = (X_{mesh} - X_{plastic})/(X_{mesh} + X_{plastic})$, where X denotes the corresponding trait value in pots under either mesh (permitting diffusive exchange between root compartments while preventing root intermingling) or plastic (isolating the two root compartments) treatments. Planting compositions denote intraspecific (monoculture) and interspecific (mixture) interactions. Bars show RII estimates, and error bars indicate percentile 95 % confidence intervals obtained from 10 000 stratified, unpaired pot-level bootstrap iterations. For monocultures, the two conspecific plants were averaged within each pot before resampling; for mixtures, species-specific observations from the same pot were retained within the same resampling cluster. Positive and negative RII estimates indicate higher and lower trait values, respectively, in the mesh treatment than in the plastic treatment. The horizontal dashed line at RII = 0 denotes no difference between barrier treatments. Confidence intervals excluding zero indicate a difference between the mesh and plastic treatments.

allocation were negative in *O. nivara* but positive in *O. sativa*, particularly under low N. Absolute trait values further distinguished changes in plant size from shifts in biomass allocation. Under low N in mixtures, *O. sativa* had similar root biomass under mesh and plastic treatments (3.91 vs 3.73 g per plant), despite lower whole-plant biomass under mesh. Its root-to-shoot ratio was therefore higher under mesh (0.242 vs 0.188), indicating greater relative root allocation rather than greater overall growth (Supplementary Data Figs S2 and S3; Supplementary Data Table S2). In contrast, under high N in mixtures, *O. nivara* had lower whole-plant and root biomass under mesh, while its root-to-shoot ratio changed little (0.141 vs 0.149), suggesting that reduced root biomass mainly reflected smaller plant size rather than altered allocation.

Root biomass components provided additional detail on how root growth responded within these whole-plant patterns (Fig. 2B, C). In *O. nivara*, scanned axial root biomass increased in monocultures under high N but decreased under low N and in mixed plantings under both N levels (Fig. 2B). In *O. sativa*, scanned axial root biomass showed no significant response in monocultures under high N, but marginally increased in monocultures under low N, decreased significantly in mixed plantings under high N, and increased again under low N. Unscanned lateral root biomass showed the most consistently negative RII estimates among the root biomass components (Fig. 2C). In *O. nivara*, it was reduced under low N in monocultures and under both N levels in mixed plantings, with the strongest suppression under low N in mixtures. In *O. sativa*, unscanned lateral root biomass was reduced in monocultures under high N and in mixed plantings under low N, but increased in monocultures under low N.

Nitrogen accumulation and partitioning

Nitrogen accumulation responses differed between the two rice species and varied with both N level and planting composition (Fig. 3). In mixtures, *O. sativa* showed RII estimates close to zero or above zero for leaf, root and total N accumulation, whereas the corresponding estimates for *O. nivara* were predominantly below zero. The difference between species was most pronounced under low N, where *O. nivara* had reduced total N accumulation, while *O. sativa* showed little reduction. Under high N, *O. sativa* still exhibited more favourable RII estimates, particularly for total and stem N accumulation, whereas *O. nivara* remained slightly negative. These results showed that N accumulation declined more strongly in *O. nivara* than in *O. sativa* when the two species were grown together.

Leaf traits and photosynthetic parameters

Leaf-level traits showed weaker and less consistent responses to mesh-mediated below-ground interactions than whole-plant biomass and N-related traits. Linear mixed-effects models showed significant main effects of species and N supply level on several leaf photosynthetic traits and chlorophyll content (Supplementary Data Table S5). However, interactive effects involving the root barrier treatment were generally absent. Among the measured leaf traits,

Downloaded from academic.oup.com/aob/advance-article/doi/10.1093/aob/mcag343/9002709 by National Science & Technology Library user on 24 November 2026

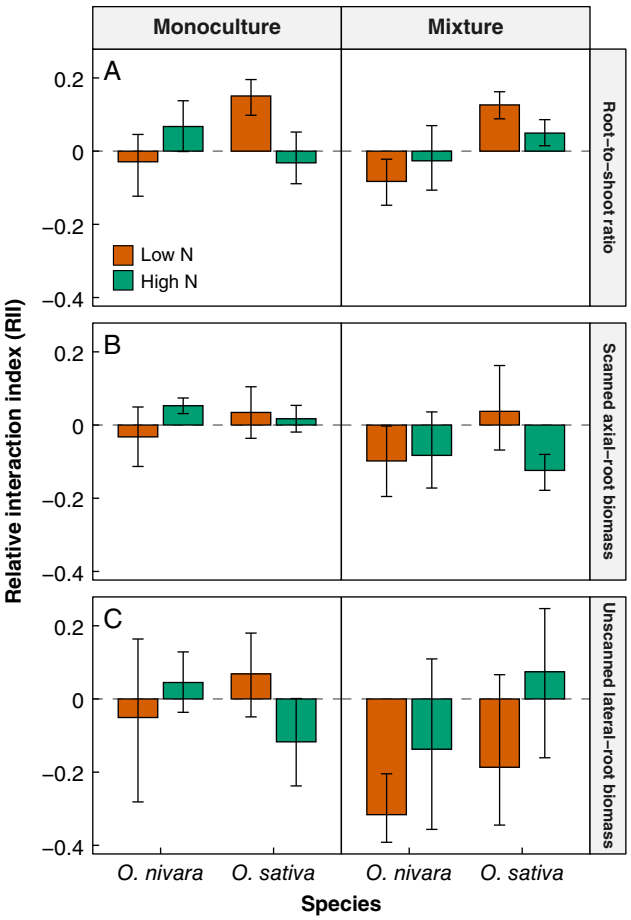


FIG. 2. Relative interaction index (RII) of biomass allocation and root biomass components under contrasting N conditions. Plant-level RII of (A) root-to-shoot ratio, (B) scanned axial root biomass, and (C) unscanned lateral root biomass for *O. sativa* and *O. nivara* grown under low and high N supply levels in monoculture and mixture treatments. The index was calculated as $RII = (X_{mesh} - X_{plastic})/(X_{mesh} + X_{plastic})$, where X denotes the corresponding trait value in pots under either mesh (permitting diffusive exchange between root compartments while preventing root intermingling) or plastic (isolating the two root compartments) treatments. Bars represent means ± 95 % confidence intervals. Positive and negative RII estimates indicate higher and lower trait values, respectively, in the mesh treatment than in the plastic treatment. The horizontal dashed line at RII = 0 denotes no difference between barrier treatments. An RII estimate was considered different from zero when its bootstrap confidence interval excluded zero.

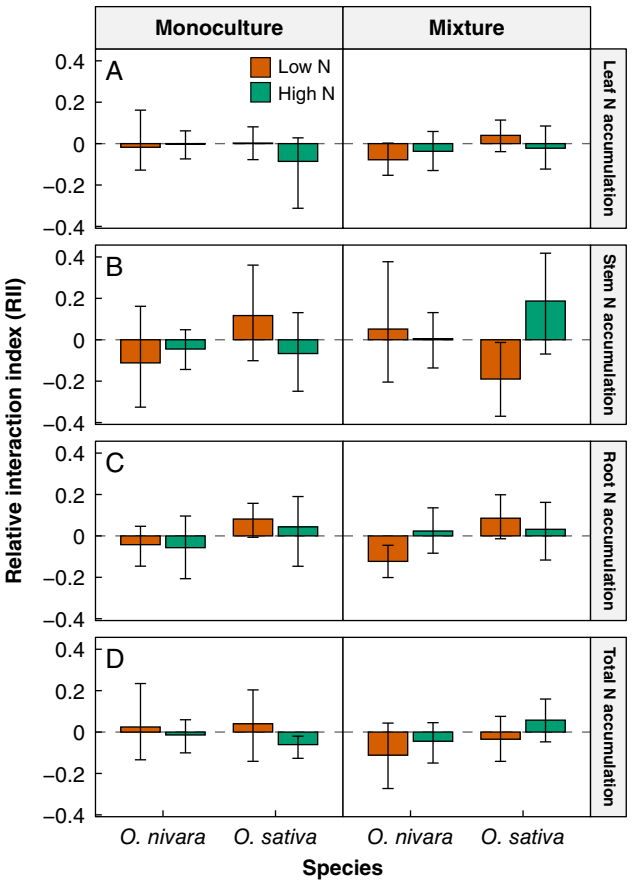


FIG. 3. Relative interaction index (RII) of nitrogen (N) accumulation under contrasting N conditions. Plant-level RII of (A) leaf N accumulation, (B) stem N accumulation, (C) root N accumulation and (D) total N accumulation for *O. sativa* and *O. nivara* grown under low and high N supply levels in monoculture and mixture treatments. The index was calculated as $RII = (X_{mesh} - X_{plastic})/(X_{mesh} + X_{plastic})$, where X denotes the corresponding trait value in pots under either mesh (permitting diffusive exchange between root compartments while preventing root intermingling) or plastic (isolating the two root compartments) treatments. Bars represent means ± 95 % confidence intervals. Positive and negative RII estimates indicate higher and lower trait values, respectively, in the mesh treatment than in the plastic treatment. The horizontal dashed line at RII = 0 denotes no difference between barrier treatments. An RII estimate was considered different from zero when its bootstrap confidence interval excluded zero.

only g_s showed a significant three-way interaction among planting composition, N supply level and root barrier treatment. No comparable interactive effects were detected for the other leaf traits. PCA summarized the major patterns of covariation among representative whole-plant, root and leaf traits (Supplementary Data Fig. S5). PC1 and PC2 explained 69.9 and 15.3 % of the total variance, respectively. PC1 was associated mainly with overall plant performance and root size traits, including total biomass, total N accumulation, leaf area per plant, tip number of the scanned root fraction and scanned axial root length, whereas PC2 was influenced primarily by leaf physiological traits, especially A and V_{cmax}. Thus, leaf physiological variables and cumulative whole-plant and root traits occupied partly different directions in multivariate trait space. This pattern was descriptive and consistent with limited coordination between instantaneous leaf physiology and cumulative growth responses.

Despite this weak overall response, planned contrasts identified several treatment-specific changes in mixtures (Supplementary Data Table S4). Under low N, *O. nivara* grown in mixtures showed higher values of several photosynthetic traits under the mesh treatment than under the plastic treatment. In this species, the RII estimates for A, g_s, V_{cmax} and J_{max} were all significantly positive (Fig. 4). For *O. sativa*, no comparable significant mesh–plastic differences were detected in A, g_s, V_{cmax}, J_{max} or the other measured leaf physiological traits under low N, and most RII estimates were close to zero. Under high N, the RII estimates for most leaf traits were neutral in both *O.nivara* and *O. sativa*. In monocultures, neither species showed clear or consistent responses of leaf photosynthetic traits to mesh-mediated below-ground interactions.

Downloaded from academic.oup.com/aob/advance-article/doi/10.1093/aob/mcag343/9002709 by National Science & Technology Library user on 24 November 2026

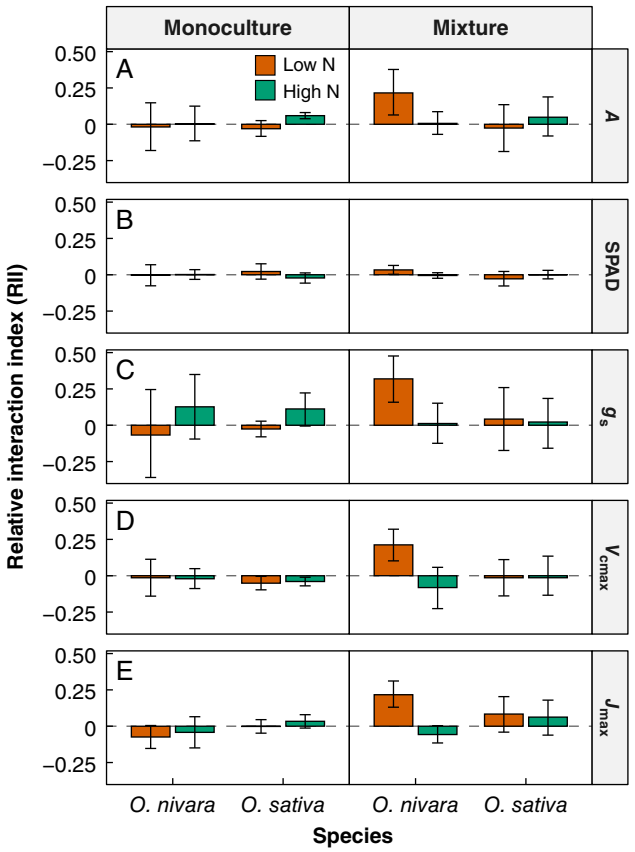


FIG. 4. Relative interaction index (RII) of leaf physiological traits under contrasting N conditions. RII of (A) net photosynthetic rate (A), (B) SPAD value, (C) stomatal conductance (g_s), (D) maximum rate of Rubisco carboxylation (V_{cmax}) and (E) maximum rate of electron transport (J_{max}) for *O. sativa* and *O. nivara* grown under low and high N supply levels in monoculture and mixture treatments. The index was calculated as RII $= (X_{mesh} - X_{plastic})/(X_{mesh} + X_{plastic})$, where X denotes the corresponding trait value in pots under either mesh (permitting diffusive exchange between root compartments while preventing root intermingling) or plastic (isolating the two root compartments) treatments. Bars represent means ± 95 % confidence intervals. Positive and negative RII estimates indicate higher and lower trait values, respectively, in the mesh treatment than in the plastic treatment. The horizontal dashed line at RII = 0 denotes no difference between barrier treatments. An RII estimate was considered different from zero when its bootstrap confidence interval excluded zero.

DISCUSSION

Nitrogen supply and neighbour identity shaped contrasting interaction outcomes

Responses to mesh-mediated below-ground interactions differed markedly between monocultures and mixtures. Positive RII estimates occurred more frequently in monocultures, whereas biomass and N accumulation generally showed negative RII estimates in mixtures, particularly under low N. Because the mesh barrier permitted diffusion of water, dissolved nutrients and soluble signals while preventing direct root intermingling (Chen *et al.*, 2021; Zhu *et al.*, 2022), RII represents the standardized net difference between the mesh and plastic treatments. Its sign does not by itself identify facilitation, competition, signalling or resource redistribution as the underlying process.

Several non-exclusive mechanisms may explain the positive responses observed in monocultures. Diffusive exchange may have reduced spatial heterogeneity in mobile soil resources by allowing their redistribution towards compartments of greater depletion (Zhang *et al.*, 2020; Ma *et al.*, 2023). This effect may have been relatively balanced between conspecific neighbours with similar resource requirements and developmental schedules. Soluble compounds released by conspecific roots may also have altered root proliferation or biomass allocation (Semchenko *et al.*, 2014; Yang *et al.*, 2018). These possibilities remain hypotheses rather than evidence of facilitation because resource movement and root-derived compounds were not measured directly. Under low N, for example, *O. sativa* increased relative root allocation and some root biomass components without a corresponding increase in total biomass. This pattern indicates a shift in resource allocation rather than a positive whole-plant growth response. Under high N, its positive biomass RII occurred without increased relative root allocation, indicating that the response to mesh-mediated below-ground interactions depended on N supply.

In mixtures, mesh-mediated below-ground interactions produced predominantly negative and asymmetrical RII estimates. Differences between the two rice types in N demand, root deployment, uptake capacity or developmental timing may have allowed resource depletion in one root compartment to affect availability in the other (Zhang *et al.*, 2020). The divergence was most apparent under low N: the *O. sativa* genotype maintained N accumulation more effectively, whereas *O. nivara* showed larger reductions in biomass and organ-level N accumulation. These patterns are consistent with unequal resource acquisition under the mesh treatment, but the experiment cannot determine whether they resulted from nutrient depletion, soluble signalling or rhizosphere-mediated processes. Distinguishing among these mechanisms will require direct measurements of soil mineral N dynamics, uptake kinetics and root-derived compounds (Semchenko *et al.*, 2014; Anten and Chen, 2021; Yu *et al.*, 2021).

Contrasting genotype responses under heterospecific below-ground interactions

The more favourable response of the *O. sativa* genotype in mixtures does not fit a simple expectation that domestication should uniformly weaken resource acquisition responses to heterospecific neighbours. Crop breeding is often assumed to favour stand-level productivity over traits that enhance individual resource pre-emption (Donald, 1968; Montazeaud *et al.*, 2020). However, domestication has altered root traits in different directions among crop species, and cultivated forms may retain or acquire traits that support nutrient capture under resource limitation (Martín-Robles *et al.*, 2019; Perkins and Lynch, 2021). The response of *O. sativa* in the present experiment may therefore reflect divergence in root allocation, nutrient demand or uptake efficiency rather than a general increase or decrease in competitiveness.

One possible explanation is that the *O. sativa* genotype had a greater N requirement and consequently expressed a

Downloaded from academic.oup.com/aob/advance-article/doi/10.1093/aob/mcag343/9002709 by National Science & Technology Library user on 24 November 2026

stronger resource acquisition response when N was limiting. Selection for high productivity may increase nutrient demand, potentially favouring stronger plastic adjustment in root allocation or N uptake under deficiency (Dissanayaka *et al.*, 2017). Alternatively, the observed difference may have arisen from variation between the two rice types in growth rate, root deployment, uptake kinetics or the efficiency with which acquired N was converted into biomass (Hajiboland *et al.*, 2009; Memon *et al.*, 2025). These mechanisms are not mutually exclusive, and the present experiment cannot distinguish among them because plant N demand, root uptake activity and soil mineral N depletion were not measured directly.

The observed pattern should therefore be interpreted cautiously. Because the experiment included only one cultivated *O. sativa* genotype with one *O. nivara* accession, the differences observed here should be considered specific to these two materials rather than species-wide differences or general effects of domestication (Chen *et al.*, 2021). The present results therefore do not demonstrate that the *O. sativa* genotype is generally more competitive than the *O. nivara* accession. Rather, they show that the *O. sativa* genotype was not disadvantaged in maintaining resource acquisition under heterospecific below-ground interactions in the conditions tested. More broadly, the contrast observed between the cultivated genotype and wild accession tested here cannot be attributed to domestication history alone and may instead reflect differences in the resource acquisition strategies expressed by these two materials under the tested nutrient conditions.

Leaf physiological responses were not consistently coordinated with whole-plant outcomes

Leaf physiological responses did not consistently parallel the cumulative changes in biomass allocation and N accumulation. Across treatments, the mesh–plastic comparison produced few consistent changes in photosynthetic rate, stomatal conductance, mesophyll conductance, chlorophyll status or biochemical photosynthetic capacity. However, these weak physiological responses should be interpreted cautiously because the response curve measurements were based on four biological replicates per treatment combination. Although measurements were restricted to newly fully expanded leaves and conducted under standardized conditions, residual variation associated with leaf developmental status, canopy position and plant-to-plant heterogeneity may have reduced statistical power to detect treatment effects. By contrast, biomass allocation, root biomass components and organ-level N accumulation showed clearer context-dependent responses. The limited correspondence between these trait classes may therefore reflect both differences in temporal and organizational scale and differences in measurement precision and statistical power (Wang *et al.*, 2021; Carter *et al.*, 2025).

The clearest mismatch between scales occurred in *O. nivara* grown in mixtures under low N. Under this treatment combination, mesh-mediated below-ground interactions reduced biomass and N accumulation, whereas several leaf physiological traits responded positively. The measured leaves therefore maintained, or perhaps transiently increased, physiological performance despite reductions in whole-plant resource acquisition. One possible explanation is compensatory adjustment, in which active leaves maintain relatively high carbon assimilation when whole-plant N capture or growth is constrained (Newingham *et al.*, 2007). Alternatively, the pattern may reflect differences in leaf developmental status, plant size or the timing of physiological acclimation (De Souza *et al.*, 2018; Wang *et al.*, 2020). Because leaf physiology was measured at only one time point, the present experiment cannot distinguish among these explanations.

The limited correspondence between leaf and whole-plant responses suggests that the effects of mesh-mediated below-ground interactions were expressed mainly through cumulative changes in resource capture and allocation rather than through consistent shifts in leaf physiological capacity. Leaf-level measurements nevertheless provided complementary information by showing that reduced biomass or N accumulation did not necessarily coincide with lower instantaneous photosynthetic performance. Repeated measurements over time, together with estimates of canopy-level carbon assimilation and leaf area development, would be required to determine whether these leaf responses were transient, compensatory or persistent (Wang, 2024; Xiong, 2024; Yan *et al.*, 2024). The cross-scale comparison therefore suggests limited correspondence between instantaneous leaf function and cumulative whole-plant outcomes, rather than demonstrating physiological decoupling between these scales.

Limitations and future directions

Several limitations should be considered. First, this study compared only one cultivated rice genotype, *O. sativa*, with *O. nivara*, a wild relative of cultivated rice. The observed differences should therefore be interpreted as specific to the cultivated rice genotype and wild accession tested here, rather than as species-wide differences or general effects of domestication. Broader sampling across cultivated varieties and multiple wild rice accessions will be required to determine whether these patterns are repeatable and whether they reflect domestication-associated divergence (Yang *et al.*, 2018; De Tombeur *et al.*, 2022). Moreover, both species belong to *Oryza* and thus represent a relatively close taxonomic comparison. Below-ground interactions with more distantly related neighbours, including other grasses or dicotyledonous species, may therefore differ from the patterns observed here.

Second, the mesh and PTFE treatments contrasted permeability and impermeable separation of the two soil compartments. The mesh permitted diffusion of water, nutrients and soluble signals while preventing direct root intermingling, whereas the PTFE film blocked both root contact and diffusive exchange (Chen *et al.*, 2021; Yang *et al.*, 2024). However, the barriers may also have differed in other physical properties. Roots could have responded differently to the nylon mesh and PTFE surfaces or to differences in local mechanical impedance. Movement of water and dissolved nutrients through the mesh may also have altered resource

Downloaded from academic.oup.com/aob/advance-article/doi/10.1093/aob/mcag343/9002709 by National Science & Technology Library user on 24 November 2026

distribution between compartments and, consequently, size asymmetry between neighbouring plants. Because biomass allocation and root traits can vary allometrically with plant size, some mesh–plastic differences may partly reflect size-dependent effects. These effects cannot be separated from diffusive exchange in the present design. The mesh–plastic contrast should therefore be interpreted as the net response to the two barrier environments rather than as a direct measure of chemical signalling or competition. Container restriction cannot be excluded because each plant was confined to one compartment of a 5.0-L pot, and roots had reached the compartment walls by harvest. Although compartment volume was standardized across treatments, the two rice types or N treatments may have differed in their sensitivity to spatial restriction (Poorter *et al.*, 2012).

Third, the mechanisms underlying the observed responses remain unresolved. This study focused on biomass, N accumulation and leaf physiology but did not directly measure soil mineral N depletion, N uptake kinetics, root exudates or rhizosphere microbial processes. Measuring these variables in future work would help clarify why the two rice types differed in N acquisition under below-ground interactions (Yang *et al.*, 2018; Anten and Chen, 2021).

Finally, leaf physiological traits were measured at a single time point, whereas biomass and N accumulation integrated responses over the growth period. Repeated physiological measurements or canopy-level photosynthesis estimates would help determine whether leaf-level responses are genuinely weak or transient (Wang, 2024; Xiong, 2024; Yan *et al.*, 2024). In addition, the time-intensive nature of A–C_i and light response curve measurements limited our biological replication ($n = 4$), which may reduce statistical power for highly variable leaf physiological traits. Field experiments or large-container experiments under more realistic paddy conditions would also help test the ecological relevance of these results (Yang *et al.*, 2018; Zhu *et al.*, 2019*b*).

Conclusions

Nitrogen supply and neighbour identity jointly influenced plant responses to mesh-mediated below-ground interactions in a cultivated rice genotype and a wild relative. The effects of mesh-mediated below-ground interactions were strongly context-dependent. Responses were neutral or positive in some monocultures but predominantly negative in mixtures, showing that interaction outcomes differed between the conspecific and heterospecific *Oryza* pairings tested here. This contrast was most pronounced under low N, when the *O. sativa* genotype and the *O. nivara* accession diverged in biomass allocation and N acquisition. In mixtures, the *O. sativa* genotype better maintained total N accumulation and increased relative root allocation, whereas the *O. nivara* accession showed larger reductions in these whole-plant traits. Leaf physiological responses were more treatment-specific and did not consistently parallel cumulative changes in biomass and N economy, suggesting limited correspondence between instantaneous leaf function and whole-plant performance. Because the experiment compared a single cultivated rice genotype with a single wild relative, these differences should not be interpreted as general effects of domestication. In addition, the mesh treatment allowed diffusive exchange between root compartments but prevented direct root intermingling. Within these limits, our results show that mesh-mediated below-ground interaction outcomes cannot be predicted from nutrient availability or neighbour identity alone. Instead, they depend on the combined effects of these factors on resource acquisition and allocation.

SUPPLEMENTARY DATA

Supplementary data are available at *Annals of Botany* online and consist of the following. Figure S1: schematic diagram of experimental planting compositions and root barrier treatments. Figure S2: pot- and plant-level total biomass responses to mesh-mediated below-ground interactions. Figure S3: root-to-shoot ratio and root biomass fraction responses to mesh-mediated below-ground interactions. Figure S4: mean A–C_i curves for *O. nivara* and *O. sativa* grown under contrasting N supply levels and planting compositions with two root barrier treatments. Figure S5: PCA of representative whole-plant, root and leaf physiological traits. Table S1: combinations of the 12 experimental pot treatments. Table S2: organ-specific biomass and root-to-shoot ratio responses of *O. sativa* and *O. nivara* to mesh-mediated below-ground interactions. Table S3: summary of ANOVA results for organ-specific biomass and root-to-shoot ratio. Table S4: leaf physiological trait responses of *O. sativa* and *O. nivara* to mesh-mediated below-ground interactions. Table S5: summary of ANOVA results for leaf physiological traits.

FUNDING

This work was supported by the Earmarked Fund for China Agriculture Research System (CARS-01), the Fourth Batch of Hubei Modern Agricultural Industry Technology System (2025HBSTX4-01) and the Fundamental Research Funds for the Central Universities (2662024QH005).

ACKNOWLEDGEMENTS

We thank Jinfang Zhao, Shunjin Zhu, Ya Zhang and Zhuo Chen for their help in conducting experiments.

CONFLICT OF INTEREST

The authors have no conflicts to declare.

AUTHOR CONTRIBUTIONS

D.X. conceived the research and supervised the study. W.C. conducted the research, analysed the data and drafted the manuscript with D.X. W.C., D.X., X.Y., X.L., F.W., J.M., Z.W., K.C., J.H. and S.P. substantively revised the paper. All authors read and approved the final manuscript.

Downloaded from academic.oup.com/aob/advance-article/doi/10.1093/aob/mcag343/9002709 by National Science & Technology Library user on 24 November 2026

DATA AVAILABILITY

The primary data supporting this study were not made publicly available at the time of publication. Data will be made available upon request to the corresponding author.

REFERENCES

Anten NPR, **Chen BJW. 2021**. Detect thy family: mechanisms, ecology and agricultural aspects of kin recognition in plants. *Plant, Cell & Environment* **44**: 1059–1071. doi:10.1111/pce.14011

Bebout J, **Loaiza J**, **Gillert A**, **Cleland E. 2026**. Trait responses to competition are mostly parallel among competitor plants but can cause convergence or divergence in key traits. *Functional Ecology* **40**: 2830–2842. doi:10.1111/1365-2435.70407

Biedrzycki ML, **Bais HP. 2010**. Kin recognition: another biological function for root secretions. *Plant Signaling & Behavior* **5**: 401–402. doi:10.4161/psb.5.4.10795

Carter TA, **Stears AE**, **Fornwalt PJ**, ***et al.* 2025**. Fine-root traits coordinate with aboveground strategies yet poorly predict species' response to spruce mortality. *Plant and Soil* **514**: 1301–1313. doi:10.1007/s11104-025-07463-x

Chen BJW, **Huang L**, **During HJ**, **Wang X**, **Wei J**, **Anten NPR. 2021**. No neighbour-induced increase in root growth of soybean and sunflower in mesh-divider experiments after controlling for nutrient concentration and soil volume. *AoB PLANTS* **13**: plab020. doi:10.1093/aobpla/plab020

Coudert Y, **Périn C**, **Courtois B**, **Khong NG**, **Gantet P. 2010**. Genetic control of root development in rice, the model cereal. *Trends in Plant Science* **15**: 219–226. doi:10.1016/j.tplants.2010.01.008

De Souza AP, **Grandis A**, **Arenque-Musa BC**, **Buckeridge MS. 2018**. Diurnal variation in gas exchange and nonstructural carbohydrates throughout sugarcane development. *Functional Plant Biology* **45**: 865–876. doi:10.1071/FP17268

De Tombeur F, **Lemoine T**, **Violle C**, ***et al.* 2022**. Nitrogen availability and plant–plant interactions drive leaf silicon concentration in wheat genotypes. *Functional Ecology* **36**: 2833–2844. doi:10.1111/1365-2435.14170

Dissanayaka DMSB, **Maruyama H**, **Nishida S**, **Tawaraya K**, **Wasaki J. 2017**. Landrace of japonica rice, Akamai exhibits enhanced root growth and efficient leaf phosphorus remobilization in response to limited phosphorus availability. *Plant and Soil* **414**: 327–338. doi:10.1007/s11104-016-3129-1

Donald CM. 1968. The breeding of crop ideotypes. *Euphytica* **17**: 385–403. doi:10.1007/BF00056241

Ehlers BK, **Bilde T. 2019**. Inclusive fitness, asymmetric competition and kin selection in plants. *Oikos* **128**: 765–774. doi:10.1111/oik.06390

Hajiboland R, **Afiasgharzad N**, **Barzeghar R. 2009**. Influence of arbuscular mycorrhizal fungi on uptake of Zn and P by two contrasting rice genotypes. *Plant, Soil and Environment* **55**: 93–100. doi:10.17221/319-PSE

Jaafry SWH, **Li D**, **Fan Z**, ***et al.* 2019**. Effect of soil nutrients, neighbor identities and root separation types on intra- and interspecific interaction among three clonal plant species. *Nordic Journal of Botany* **37**: njb.02070. doi:10.1111/njb.02070

Kiba T, **Krapp A. 2016**. Plant nitrogen acquisition under low availability: regulation of uptake and root architecture. *Plant & Cell Physiology* **57**: 707–714. doi:10.1093/pcp/pcw052

Lai Z, **Liao Z**, **Kou H**, ***et al.* 2026**. From acquisition to conservation: whole-plant trait coordination under water-nitrogen interactions determines maize yield and water productivity. *European Journal of Agronomy* **177**: 128114. doi:10.1016/j.eja.2026.128114

Ma X, **Yu W**, **Tao M**, ***et al.* 2023**. Clonal integration in *Vallisneria natans* alters growth and the rhizosphere microbial community of neighboring plants under heterogeneous conditions. *Plant and Soil* **482**: 297–311. doi:10.1007/s11104-022-05690-0

Mahaut L, **Violle C**, **Shihan A**, ***et al.* 2023**. Beyond trait distances: functional distinctiveness captures the outcome of plant competition. *Functional Ecology* **37**: 2399–2412. doi:10.1111/1365-2435.14397

Martín-Robles N, **Morente-López J**, **Freschet GT**, **Poorter H**, **Roumet C**, **Milla R. 2019**. Root traits of herbaceous crops: pre-adaptation to cultivation or evolution under domestication? *Functional Ecology* **33**: 273–285. doi:10.1111/1365-2435.13231

Mazal L, **Fajardo A**, **Till-Bottraud I**, **Corenblit D**, **Fumanal B. 2023**. Kin selection, kin recognition and kin discrimination in plants revisited: a claim for considering environmental and genetic variability. *Plant, Cell & Environment* **46**: 2007–2016. doi:10.1111/pce.14584

Memon SUR, **Memon SP**, **Qasim M**, ***et al.* 2025**. Comparative efficacy of different rice (*Oryza sativa* L.) genotypes for improved zinc and iron uptake and relevant yield efficiency under their foliar application. *Journal of Soil Science and Plant Nutrition* **25**: 6861–6871. doi:10.1007/s42729-025-02567-w

Minden V, **Olde Venterink H. 2019**. Plant traits and species interactions along gradients of N, P and K availabilities. *Functional Ecology* **33**: 1611–1626. doi:10.1111/1365-2435.13387

Montazeaud G, **Rousset F**, **Fort F**, **Violle C**, **Fréville H**, **Gandon S. 2020**. Farming plant cooperation in crops. *Proceedings of the Royal Society of London B* **287**: 20191290. doi:10.1098/rspb.2019.1290

Newingham BA, **Callaway RM**, **BassiriRad H. 2007**. Allocating nitrogen away from a herbivore: a novel compensatory response to root herbivory. *Oecologia* **153**: 913–920. doi:10.1007/s00442-007-0791-2

Odone A, **Thorup-Kristensen K. 2025**. Modern wheat has deeper roots than ancient wheats: is this an adaptation to higher productivity? *Annals of Botany* **136**: 1193–1201. doi:10.1093/aob/mcaf065

Perkins AC, **Lynch JP. 2021**. Increased seminal root number associated with domestication improves nitrogen and phosphorus acquisition in maize seedlings. *Annals of Botany* **128**: 453–468. doi:10.1093/aob/mcab074

Poorter H, **Fiorani F**, **Stitt M**, ***et al.* 2012**. The art of growing plants for experimental purposes: a practical guide for the plant biologist. *Functional Plant Biology* **39**: 821–838. doi:10.1071/FP12028

Semchenko M, **Saar S**, **Lepik A. 2014**. Plant root exudates mediate neighbour recognition and trigger complex behavioural changes. *New Phytologist* **204**: 631–637. doi:10.1111/nph.12930

Wang B, **Cai W**, **Li J**, ***et al.* 2020**. Leaf photosynthesis and stomatal conductance acclimate to elevated [CO_2] and temperature thus increasing dry matter productivity in a double rice cropping system. *Field Crops Research* **248**: 107735. doi:10.1016/j.fcr.2020.107735

Wang S, **Li L**, **Zhou D. 2021**. Root morphological responses to population density vary with soil conditions and growth stages: the complexity of density effects. *Ecology and Evolution* **11**: 10590–10599. doi:10.1002/ece3.7868

Wang X, **An Y**, **Wang L**, ***et al.* 2026**. Leaf and root traits codetermine biomass production and allocation patterns in agriculturally managed wetlands in a semi-arid region. *Agriculture, Ecosystems & Environment* **400**: 110229. doi:10.1016/j.agee.2026.110229

Wang Y. 2024. Improving photosynthetic efficiency in fluctuating light to enhance yield of C_3 and C_4 crops. *Crop and Environment* **3**: 184–193. doi:10.1016/j.crope.2024.06.003

Weiner J, **Du Y**, **Zhang C**, **Qin X**, **Li F. 2017**. Evolutionary agroecology: individual fitness and population yield in wheat (*Triticum aestivum*). *Ecology* **98**: 2261–2266. doi:10.1002/ecy.1934

Xiong D, **Liu X**, **Liu L**, ***et al.* 2015**. Rapid responses of mesophyll conductance to changes of CO_2 concentration, temperature and irradiance are affected by N supplements in rice. *Plant, Cell & Environment* **38**: 2541-2550. doi:10.1111/pce.12558

Xiong D, **Flexas J**, **Yu T**, **Peng S**, **Huang J. 2017**. Leaf anatomy mediates coordination of leaf hydraulic conductance and mesophyll conductance to CO_2 in *Oryza*. *New Phytologist* **213**: 572–583. doi:10.1111/nph.14186

Xiong D. 2024. Perspectives of improving rice photosynthesis for higher grain yield. *Crop and Environment* **3**: 123–137. doi:10.1016/j.crope.2024.04.001

Xu C, **Zhang M**, **Liu M**, **An S**, **Sheng S. 2012**. Interspecific effects on plant size inequality: evidence from a temperate savanna community. *Plant Ecology* **213**: 225–235. doi:10.1007/s11258-011-0018-9

Xu Y, **Cheng H**, **Kong C**, **Meiners SJ. 2021**. Intra-specific kin recognition contributes to inter-specific allelopathy: a case study of allelopathic rice interference with paddy weeds. *Plant, Cell & Environment* **44**: 3479–3491. doi:10.1111/pce.14083

Yan Y, **Duan F**, **Li X**, ***et al.* 2024**. Photosynthetic capacity and assimilate transport of the lower canopy influence maize yield under high planting density. *Plant Physiology* **195**: 2652–2667. doi:10.1093/plphys/kiae204

Downloaded from academic.oup.com/aob/advance-article/doi/10.1093/aob/mcag343/9002709 by National Science & Technology Library user on 24 November 2026

Yang S, **Yi L**, **Wang J**, **Li X**, **Xu B**, **Liu M. 2024**. Nitrogen addition affected the root competition in *Cunninghamia lanceolata–Phoebe chekiangensis* mixed plantation. *Physiologia Plantarum* **176**: e14268. doi:10.1111/ppl.14268

Yang X, **Li L**, **Xu Y**, **Kong C. 2018**. Kin recognition in rice (*Oryza sativa*) lines. *New Phytologist* **220**: 567–578. doi:10.1111/nph.15296

Yu R-P, **Lambers H**, **Callaway RM**, **Wright AJ**, **Li L. 2021**. Belowground facilitation and trait matching: two or three to tango? *Trends in Plant Science* **26**: 1227–1235. doi:10.1016/j.tplants.2021.07.014

Zhang D, **Lyu Y**, **Li H**, ***et al.* 2020**. Neighbouring plants modify maize root foraging for phosphorus: coupling nutrients and neighbours for improved nutrient-use efficiency. *New Phytologist* **226**: 244–253. doi:10.1111/nph.16206

Zhu S-G, **Cheng Z-G**, **Yin H-H**, ***et al.* 2022**. Transition in plant–plant facilitation in response to soil water and phosphorus availability in a legume-cereal intercropping system. *BMC Plant Biology* **22**: 311. doi:10.1186/s12870-022-03706-6

Zhu Y, **Weiner J**, **Li F-M. 2019*a***. Root proliferation in response to neighbouring roots in wheat (*Triticum aestivum*). *Basic and Applied Ecology* **39**: 10–14. doi:10.1016/j.baae.2019.07.001

Zhu Y, **Weiner J**, **Yu M**, **Li F. 2019*b***. Evolutionary agroecology: trends in root architecture during wheat breeding. *Evolutionary Applications* **12**: 733–743. doi:10.1111/eva.12749

Downloaded from academic.oup.com/aob/advance-article/doi/10.1093/aob/mcag343/9002709 by National Science & Technology Library user on 24 November 2026